NeuroImage 229 (2021) 117725

Contents lists available at ScienceDirect

NeuroImage

journal homepage: www.elsevier.com/locate/neuroimage

The neural substrates of subliminal attentional bias and reduced inhibition in individuals with a higher BMI: A VBM and resting state connectivity study

S.A. Osimo [a,*], L. Piretti [a,b,c], S. Ionta [d], R.I. Rumiati [a], M. Aiello [a]

[a] Cognitive Neuroscience Department, SISSA, via Bonomea 265, 34136 Trieste, Italy
[b] Department of Psychology and Cognitive Sciences, University of Trento, corso Bettini 84, 38068 Rovereto, Italy
[c] Fondazione ONLUS Marica De Vincenzi, via Alessandro Manzoni, 11, 38122 Rovereto, Italy
[d] Sensory-Motor Lab (SeMoLa), Department of Ophthalmology, University of Lausanne, Jules Gonin Eye Hospital, Fondation Asile des Aveugles, Av. de France 15, 1002 Lausanne, Switzerland

ARTICLE INFO

Keywords:
Subliminal attention
Inhibition
Food
Obesity
Voxel-based morphometry
Resting-state connectivity

ABSTRACT

Previous studies have shown that individuals with overweight and obesity may experience attentional biases and reduced inhibition toward food stimuli. However, evidence is scarce as to whether the attentional bias is present even before stimuli are consciously recognized. Moreover, it is not known whether or not differences in the underlying brain morphometry and connectivity may co-occur with attentional bias and impulsivity towards food in individuals with different BMIs. To address these questions, we asked fifty-three participants (age $M = 23.2$, $SD = 2.9$, 13 males) to perform a breaking Continuous Flash Suppression (bCFS) task to measure the speed of subliminal processing, and a Go/No-Go task to measure inhibition, using food and nonfood stimuli. We collected whole-brain structural magnetic resonance images and functional resting-state activity. A higher BMI predicted slower subliminal processing of images independently of the type of stimulus (food or nonfood, $p = 0.001$, $\varepsilon_p{}^2 = 0.17$). This higher threshold of awareness is linked to lower grey matter (GM) density of key areas involved in awareness, high-level sensory integration, and reward, such as the orbitofrontal cortex [$t = 4.55$, $p = 0.003$], the right temporal areas [$t = 4.18$, $p = 0.002$], the operculum and insula [$t = 4.14$, $p = 0.005$] only in individuals with a higher BMI. In addition, individuals with a higher BMI exhibit a specific reduced inhibition to food in the Go/No-Go task [$p = 0.02$, $\varepsilon_p{}^2 = 0.02$], which is associated with lower GM density in reward brain regions [orbital gyrus, $t = 4.97$, $p = 0.005$, and parietal operculum, $t = 5.14$, $p < 0.001$] and lower resting-state connectivity of the orbital gyrus to visual areas [fusiform gyrus, $t = -4.64$, $p < 0.001$ and bilateral occipital cortex, $t = -4.51$, $p < 0.001$ and $t = -4.34$, $p < 0.001$]. Therefore, a higher BMI is predictive of non food-specific slower visual subliminal processing, which is linked to morphological alterations of key areas involved in awareness, high-level sensory integration, and reward. At a late, conscious stage of visual processing a higher BMI is associated with a specific bias towards food and with lower GM density in reward brain regions. Finally, independently of BMI, volumetric variations and connectivity patterns in different brain regions are associated with variability in bCFS and Go/No-Go performances.

1. Introduction

An attentional bias consists of the preferential allocation of attention to specific salient stimuli in the environment. Several conditions, such as addiction and anxiety, have been associated with a bias in the processing of symptom-related cues (Field and Cox, 2008; Bar-Haim et al., 2007). In particular, attentional biases towards food have been repeatedly observed in individuals with obesity and overweight (Brooks et al., 2011; Castellanos et al., 2009; Hendrikse et al., 2015). When shown food pictures, individuals with overweight/obesity have been reported to direct their initial gaze more often towards them than individuals with a healthy weight, even though they later show a tendency to avoid looking at them (Werthmann et al., 2015). This approach/avoidance behavior suggests that an initial automatic attentional engagement of attention in food observation is then followed by a later top-down driven food avoidance, reflecting different alterations involving early and late attentional components (Kemps and Tiggemann, 2015; Veenstra et al., 2010; Werthmann et al., 2015). The early attentional capture could be one of the causes leading to obesity, as an early attentional bias toward

* Corresponding author.
E-mail address: sofia.osimo@gmail.com (S.A. Osimo).

https://doi.org/10.1016/j.neuroimage.2021.117725
Received 3 September 2020; Received in revised form 25 December 2020; Accepted 30 December 2020
Available online 20 January 2021

unhealthy foods is predictive of an increase in BMI (Calitri et al., 2010), while attentional re-training has been shown to reduce attentional bias and consumption of high-calorie food (Zhang et al., 2018).

Crucially, salient stimuli in the environment are detected and processed even when they are presented subliminally (Bogler et al., 2011; Schmack et al., 2016; Straube et al., 2006). Exposure to subliminal arousing stimuli has been shown to elicit activation of a network incorporating primary visual areas, somatosensory, implicit memory, and conflict monitoring regions that has been proposed as a core neuronal arousal in the brain which may be at first independent of conscious processing (Brooks et al., 2012). To date, only a few studies have investigated whether individuals with overweight/obesity have an attentional bias towards food even before it is consciously recognized. For instance, Cserjesi et al. (2016) found that, compared with healthy-weighted controls, individuals with overweight/obesity show an implicit preference for large food portions, which is not matched with their explicit evaluation of food portions. In contrast, we recently observed an attentional bias toward food in individuals with a higher BMI at a late stage of stimulus processing, but not at an early one (Osimo et al., 2019). In that study, we investigated subliminal processing and reduced inhibition towards food in a sample of individuals with different BMIs, ranging from underweight to obesity. We used a breaking Continuous Flash Suppression task (bCFS) and a Go/No-Go task. Breaking CFS is a technique of binocular rivalry that measures the processing times of different stimuli at a subliminal level of processing (Tsuchiya and Koch, 2005). Faster stimulus processing time is interpreted as reflecting faster access to consciousness. Importantly, it has been shown that personal features that alter stimuli relevance influence suppression times (Schmack et al., 2016), and that clinical disorders, such as anxiety and depression, can influence suppression times of disorder-related stimuli (Capitão et al., 2014; Yang et al., 2011). The Go/No-Go task is a well-established paradigm to measure attention and response inhibition towards a stimulus category (Schulz et al., 2007); within this task, participants with overweight/obesity frequently show worse performance than controls when inhibiting responses toward food (Kulendran et al., 2017; Price et al., 2015; Svaldi et al., 2015; but see Loeber et al., 2013; Bartholdy et al., 2016; Aiello et al., 2018). Using these tasks, we observed that a higher BMI was associated with a bias toward food only in the Go/No-Go task, and with prolonged subliminal processing in the CFS task which, however, was independent of the type of stimulus (Osimo et al., 2019). Hence, the question about the extent to which the attentional bias of individuals with a higher BMI also extends to subliminal unconscious food stimuli requires further investigations.

The aim of this study was to confirm and extend our prior results in a sample of individuals with different BMIs, by also investigating the neural correlates of subliminal attentional biases and inhibition reduction using both voxel-based morphometry (VBM) and resting-state functional connectivity (RSFC). While the neural underpinnings of reduced inhibitory control have already been studied in individuals with different BMIs, showing a correlation between reduced behavioral inhibition and reduced activation of frontal inhibitory regions in individuals with overweight/obesity (Batterink et al., 2010), evidence is still lacking concerning the neural bases of subliminal processing of food stimuli in individuals with overweight and obesity. It has been shown that suppressed images are masked at the site of interocular competition and result in lower activation of early visual areas (Yuval-Greenberg and Heeger, 2013). However, the suppressed information travels beyond lower-level visual areas, and high-level information on the semantic content or motor affordances of the shown images reach areas responsible for high-level sensory integration, such as the fusiform face, parahippocampal place areas, and dorsal regions (Fang and He, 2005; Sterzer et al., 2008). Also, the time that it takes for stimuli to break suppression has been related to the activation of the occipitotemporal and orbitofrontal cortex, suggesting a crucial role of these high-level cortical regions devoted to reward in processing the preconscious affective salience of the stimulus and in influencing the speed of visual awareness through top-down modulation of visual areas (Schmack et al., 2016). Crucially, we recently found that the excitatory modulation of the right prefrontal cortex, a high-level cortical region involved in awareness (Dehaene and Changeux, 2011), reduces detection times in the bCFS tasks especially in individuals with a higher BMI (Osimo et al., 2019). On this basis, we expect to replicate the result that higher BMI correlates with slower subliminal processing and reduced inhibition. We predict that reduced inhibition at the Go/No-Go task will be linked to lower GM density and reduced connectivity of frontal regions (Batterink et al., 2010), and that behavioral differences in suppression times in the CFS task in individuals with a higher BMI will be reflected in lower GM density and connectivity of frontal control and reward regions, such as the prefrontal cortex and the orbitofrontal cortex.

2.Methods

2.1. Participants

Fifty-three participants (thirteen males) aged 19-33 years ($M = 23.2$, $SD = 2.9$) with normal or corrected-to-normal eyesight took part in the study. Participants were recruited on a volunteer basis through advertisements on different internet platforms. Potential participants were screened for conditions incompatible with MRI scanning, such as metal prostheses, pregnancy, and cardiopathy, as well as for color blindness and strabismus. Participants filled the EAT-26 questionnaire, assessing their risk of having an eating disorder (Dotti and Lazzari, 1998; Garner et al., 1982), and reported their BMI.

The EAT-26 questionnaire is a measure often used to detect the presence of eating disorders also in non-clinical populations (Anstine and Grinenko, 2000); following the scoring system of Garner et al (1982) scores range from 0 to 56, and individuals with a score above 20 are considered at risk for eating disorders. One participant was excluded from analyses for not completing the tasks correctly. The final sample included fifty-two participants: 12% underweight, 67% normal weight, 15% overweight, and 6% obese. The participants' median BMI was 22.2. Shapiro-Wilk's tests results showed that participants' BMI and EAT-26 scores were not normally distributed ($W = 0.834$, $p < 0.001$ and $W = 0.845$, $p < 0.001$, respectively). Participants also rated their hunger level on a Likert scale from 1 to 7 and reported how much time had passed since their previous meal. Table 1 summarizes the demographical data of the experimental sample in participants with a BMI higher than the median ("Higher BMI group") and lower than the median ("Lower BMI group").

Participants were tested at Udine's Santa Maria della Misericordia Hospital. This study was approved by SISSA's Ethics Committee (protocol number 8414-III 13) and by Friuli Venezia Giulia Ethics' Committee (protocol number 28311). All participants signed a consent form. This study was carried out in accordance with the Code of Ethics of the World Medical Association (Declaration of Helsinki).

2.2. Behavioral tasks

The behavioral tasks were run outside the scanner in a quiet, dedicated room inside the hospital, on the same day that the acquisition of the imaging data took place. All experimental tasks were run on a notebook computer with Windows XP. Stimuli were displayed on a 17" LCD monitor with a resolution of 1280 × 1024 pixels and a refresh rate of 60 Hz, positioned 50 cm away from participants' eyes. A chin rest was used to minimize head movements. Participants completed the bCFS and the Go/No-Go task, always in this order. The order of the tasks was kept constant to avoid consciously viewing food stimuli in the Go/No-Go task to prime subliminal processing of food in the bCFS task. The tasks and stimuli were taken from Osimo et al. (2019).

Table 1
Demographic data of the experimental sample.

	Lower BMI group (n=26)		Higher BMI group (n=26)		Group comparison
	Mean (SD)	range	Mean (SD)	Range	
Age	22.6 (2.7)	19-28	23.7 (3.2)	20-33	t(48.65)=1.328, $p = 0.191$
Body Mass Index (BMI)	19.9 (1.6)	15.3-22	26.0 (4.6)	22.3-41.9	t(30.76)=6.391, $p < 0.001$
Eating Attitudes Test-26 (EAT-26)	12.3 (14.9)	0-56	10.9 (9.1)	0-29	t(41.29)=-0.394, $p = 0.696$
Hunger level	2.58 (1.2)	1-5	2.69 (1.7)	1-6	t(44.5)= 0.278, $p = 0.78$
Time since last meal	3.96 (4.2)	0.5-17	3.02 (2.9)	0-13	t(44.1)= -0.946, $p = 0.35$
Corrected vision	14/26	18/26	[$\chi^2(1)$=0.731, $p = 0.39$		

The data is shown separately for the lower and higher BMI groups, subsets of the data obtained splitting the sample according to the BMI's median. EAT-26 scores above 20 are indicative of risk for eating disorders.

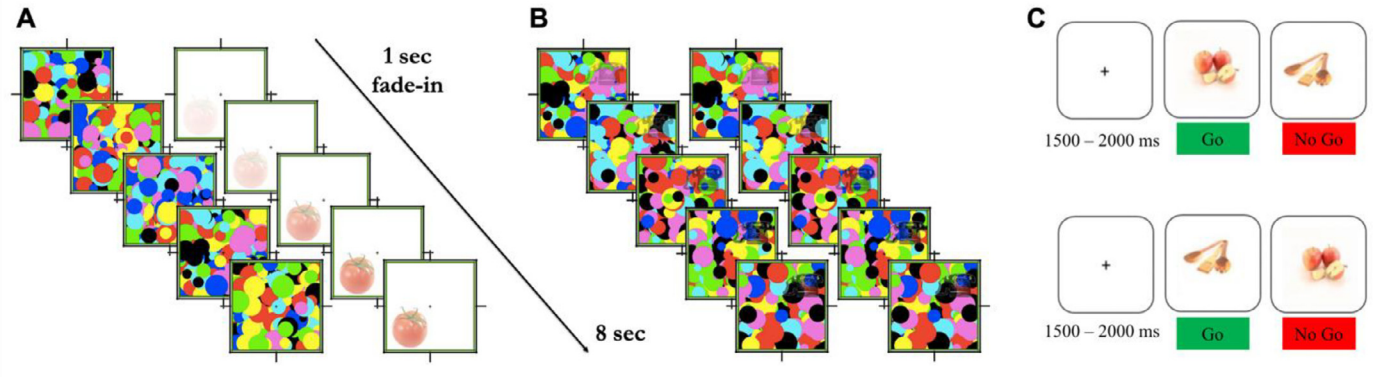

Fig. 1. An example trial of the bCFS task (A), of the NoCFS task (B), and of the Go/No-Go task in a block using food images as Go cues (above) and in a block using nonfood pictures as Go cues (below). Panel C is adapted from Aiello et al. 2017.

2.2.1. Procedure and experimental tasks

Breaking CFS and NoCFS tasks: Breaking CFS task is a binocular rivalry task, during which participants are instructed to detect and respond to static (suppressed) images while ignoring distractors. To achieve suppression, stimuli and distracters were each embedded in separate square frames and shown side by side on the screen. Stimuli were displayed in one of the quadrants of one square, while the distractors were displayed over the whole other square. Participants looked at the screen through a mirror stereoscope, which was individually calibrated to show the two squares as superimposed. Therefore, participants' perception was that of a single superimposed and perfectly aligned square. This triggered binocular rivalry, as the two eyes received different inputs in the same field of view. Participants were instructed to indicate via keypress as fast and as accurately as possible the position of the stimulus relative to a central fixation cross. Distractors were shown at 100% contrast and changed at a rate of 10 Hz, while the contrast of the stimuli increased linearly from 0% to 60% over one second, and then stayed at 60% until response. The order of the stimuli, the quadrant in which they were shown, and the eye they were shown to, were semi-randomized for each trial and each participant. Each participant saw each stimulus twice in all four quadrants in a different order and saw half of the stimuli with their right eye, and half with their left eye. Trials ended when a response was given, or, in its absence, after eight seconds. Participants then performed an equivalent task without suppression, hence NoCFS. This task had the same instructions and stimuli as the bCFS task, but stimuli and distractors were superimposed and shown to both eyes, and therefore they did not elicit binocular rivalry and were immediately visible. Participants performed 40 trials of training, during which a dedicated set of images was displayed, and 320 trials of the bCFS task and NoCFS task each, with a break every 30 trials. The total testing time was of about one hour and 15 minutes. Example trials of the bCFS and NoCFS tasks are shown in Fig. 1A and 1B. The tasks were programmed in and presented with Python using the Psychopy library (Peirce, 2007). Stimuli consisted of 20 images of food and 20 images of nonfood items (e.g. animals, man-made objects, etc.), selected from the FRIDa database (Foroni et al., 2013). Half of the food stimuli depicted highly caloric food (i.e. cookies), and the other half low-calorie foods (i.e. strawberries); in each group, half of the depicted foods were highly transformed (ice cream, fruit salad) and the other half was comprised of natural foods (almonds, cherries). Food and nonfood items were matched for brightness [p= 0.82] and spatial frequency [$p = 0.09$] since low-level visual features can influence suppression times (Gayet et al., 2014; Gray et al., 2013; Yang and Blake, 2012). Food and nonfood items also did not differ in valence, familiarity, typicality, or arousal according to the database-independent ratings [$ps > 0.15$]. A subset of the stimuli is depicted in Supplementary Figure 1. The distractor images consisted of a set of 100 pictures with colorful oval shapes of different sizes creating random patterns.

Go/No-Go task: Participants were instructed to respond as quickly as possible to Go stimuli and to refrain from responding when a No-Go stimulus was presented. In half of the blocks, Go cues consisted of food images and No-Go cues of nonfood images (depicting kitchen utensils), while in the other half the assignment was reversed. There were four blocks of 40 trials each. In each block, 12 out of 40 trials (30%) were No-Go trials. The Go/No-Go task and the stimuli were the same as those used by Aiello et al. (2017). The order of the blocks was semi-random (ABAB or BABA) and changed across sessions and participants. An example trial is depicted in Fig. 1C.

2.2.2. Analyses

Breaking continuous flash suppression: We investigated the effect of the participants' BMI on RTs in the bCFS and NoCFS tasks using linear mixed-effects models (LMMs). All analyses were run using the software R (version 3.6.2, R Core Team, 2017). LMMs were tested using the "lmer" function (lme4 package, Bates et al., 2015). Effect sizes of the LMMs were calculated using the marginal and conditional R2 statistics (Draper and Smith, 1998) using the r.squaredGLMM function of the MuMIn package (Barton, 2020). The effect size of individual factors

was calculates using the effectsize package (Ben-Shachar et al., 2020). Marginal R2 statistics quantify the amount of variance explained by the fixed effects of the models, while conditional R2 quantifies the variance explained by both fixed and random effects. Reaction times were cleaned by removing trials with no responses (12.79% across all participants), wrong responses (1.35%), with RTs below 500 ms (0.19%), and with RTs that were more than 2.5 SD from the mean of each subject (0.02%). RTs were log-transformed, and BMI and EAT-26 scores were mean-centered. Summary statistics on the included and excluded trials are reported in Supplementary Table 1.

The initial model investigating the effect of participants' BMI on the reaction times of the bCFS and NoCFS tasks, derived from the experimental hypothesis, included Task (bCFS, NoCFS), Stimulus Type (Food, NonFood), and BMI as predictors, and Participant, Image, Stimulus Location and Age as random intercepts. To control for the effect of dysfunctional eating habits on attentional bias and inhibition, EAT-26 scores were covaried in all models. To verify that all predictors and all interactions significantly improved the model fit, non-significant interactions and predictors were removed from the model, and the resulting model was compared to the initial model on the basis of the AIC criterion (Bolker et al., 2009), using the "anova" function (lmerTest package, Kuznetsova et al., 2017). All factors and interactions that did not significantly improve the initial model were pruned. To confirm that high-level interactions explained more variance than the combination of the lower-level interactions, we compared the AIC of models with and models without the high-level interactions, and only included high-level interactions that improved the models' fit.

To make sure our predictors were not correlated among themselves, we computed the variance inflation factor (VIF) for the predictors of the final model using the VIF function of the car package (Fox and Weisberg, 2019). All VIF values were between 1 and 4, indicating low collinearity among predictors.

The final model included Task, BMI, and Stimulus Type as predictors, and the interactions between Task and BMI and Task and Stimulus Type. The comparison between the initial and final model is reported in Supplementary Table 2.

Go/No-Go task: As in the bCFS and NoCFS tasks, we used linear mixed-effects models (LMMs) to calculate the effect of the participants' BMI on RTs in the Go/No-Go task. One participant was excluded from the analyses for omitting to respond in a fourth of the trials. To calculate the effect of the participants' BMI on accuracy, we used a general linear mixed model (GLMM) fitted on binomial data. LMMs were tested using the "lmer" function, and the GLMM using the "glmer" function (lme4 package, Bates et al., 2015). In the analysis of the RTs of the Go trials, only correct responses that did not deviate more than 2.5 SD from each participants' mean were included (wrong responses = 1,89%, outlier responses = 0.03%). RTs were log-transformed, and BMI and EAT-26 scores were mean-centered. Accuracy in the Go/No-Go task was coded as a binomial variable (1 = correct response, 0 = wrong response). Summary statistics on the included and excluded trials are reported in Supplementary Table 1.

In the analysis regarding the effect of BMI on the RTs in the Go/No-Go task, the initial model included Stimulus Type and BMI as predictors, and Participant, Image, and Age as random intercepts. EAT-26 scores were covaried. The same stepwise procedure used in the analyses of RTs in the bCFS and NoCFS tasks was adopted to make sure all factors increased the models' fit. The final model included only Stimulus Type, BMI, and their interaction as predictors. In the analysis on accuracy, the initial model included Trial Type (Go, NoGo), Stimulus Type and BMI as predictors, EAT-26 scores as a covariate, and Participant, Image, and Age as random intercepts. The final model only included Trial Type as a predictor and EAT-26 scores as a covariate. Variance inflation factors (VIF) for the predictors of the final models were between 1 and 2, indicating low collinearity among predictors.

All comparisons between initial and final models are reported in Supplementary Table 2.

2.3. Imaging

2.3.1. Data acquisition and preprocessing

A 3 Tesla Philips Achieva scanner was used to acquire the anatomical and functional images. Anatomical images consisted of high-resolution T_1-weighted images [brain scan acquired along the AC-PC plane, 170 sagittal slices, FOV = 176 × 240 × 240 mm, voxel size = 1 × 1 × 1 mm, reconstruction matrix = 256 × 256, flip angle = 12°, TR = 8.1 ms, TE = 3.7 ms]. For the functional data acquisition, participants were asked to relax and keep their eyes open. No stimulus was displayed during this time. The scan lasted 8 minutes. Functional $T_2{}^*$-weighted echo planar images were acquired over 36 transverse slices of 3 mm slice thickness using a single-shot pulse sequence [slice order interleaved, FOV = 230 × 230 × 108 mm, acquired voxel size = 3.59 × 3.71 × 3.00 mm, reconstructed voxel size = 3.59 × 3.59 × 3.00 mm,acquisition matrix = 64 × 62, flip angle = 90°, TR = 2500 ms, TE = 35 ms].

In the VBM analyses, preprocessing was done using the SPM12 (version 7219, Friston et al., 2017) and CAT12 (version 12.3, r1318; Gaser and Danhke, 2016) toolboxes in Matlab (version 2017a, 9.2.0, www.mathworks.com/products/matlab.html). Scans were spatially normalized using the DARTEL algorithm, and SPM12 tissue probability maps were used to segment the scans into grey matter (GW), white matter (WM), and cerebrospinal fluid (CSF), as well as for spatial registration, after which the Total Intracranial Volume (TIV) was calculated. Data were then smoothed with an 8 mm full width at half maximum (FWHM) gaussian kernel. The final voxel size was of 1.5 × 1.5 × 1.5 mm. For the resting state analyses, data were preprocessed and analyzed using the CONN toolbox (version 17; Whitfield-Gabrieli and Nieto-Castanon, 2012). The preprocessing was done following CONN's default processing pipeline. Raw functional images were realigned and unwarped, time-slice corrected, and coregistered to T_1 weighted images. Images were then normalized in MNI space and spatially smoothed with an 8 mm FWHM kernel. Data were processed by removing movement parameters by covarying the 6 rotation/translation movement, as well as regressing motion outliers using the ART package (Artifact Detection Tools, https://www.nitrc.org/projects/artifact_detect). Following the standard settings implemented in CONN, no participant was discarded from the analysis, since acquisition's frame-wise displacements were below 0.9 mm and global BOLD signal changes were below 5 SD for all participants. In addition, other sources of noise were estimated by extracting the average BOLD time series from seeds located within the white matter and CSF areas, and the first five components of the signal were regressed out, following CONN's default processing pipeline (Whitfield-Gabrieli and Nieto-Castanon, 2012). Finally, the BOLD signal was band-pass filtered (.008 Hz–.09 Hz).

2.3.2. VBM analyses

The VBM analyses were designed to investigate three main experimental questions. The *first* experimental question was whether GM density in specific brain areas significantly correlated with participants' performance on the bCFS and Go/No-Go tasks. *Secondly*, we investigated whether GM concentration in specific brain areas correlated with participants' BMI. *Finally*, when BMI influenced participants' performance, we aimed to explore the connection between task performance and BMI, i.e. whether participants' performance in the behavioral tasks predicted GM density differently in participants with a lower and with a higher BMI. To answer these experimental questions, we ran a series of multiple regressions using SPM12 (Friston et al., 2017). In the first level analyses, the preprocessed fMRI data were entered into a bivariate correlation. In all models, age, gender, and total intracranial volume (TIV) were covaried. Regressors were mean-centered.

In the model regarding the correlation between GM density and performance at bCFS task, the covariate variable was calculated as the mean suppression times in the bCFS task for each participant, normalized by their RTs in the NoCFS task, to account for differences in response times that are not due to longer suppression. In the models of the Go/No-

Go task, we used as predictors of general performance the mean of the RTs on Go trials and the number of false alarms on No-Go trials. The models investigating a specific attentional bias towards food used the difference between the mean nonfood and food RTs on Go trials. Secondly, we investigated whether participants' BMI significantly predicted GM density in any brain area. Finally, to assess whether in participants with a higher BMI, compared to participants with a lower BMI, performance in the behavioral tasks was connected to GM density in different areas, we formed two groups of participants, one with higher BMIs and one with lower BMIs, based on a median split. We ran two full factorial models with suppression times in the CFS task and the mean difference between nonfood and food RTs in Go trials in the Go/No-Go trials as behavioral covariates to assess whether a significantly different regression slope predicted GM density in the two groups, based on their behavioral performance. The regression slopes' beta values were extracted using the REX Matlab toolkit (Duff et al., 2007). Corrections for multiple comparisons based on uncorrected voxel-level (alpha = 0.001) and Family-Wise Error Rate (FWE) at a cluster level (alpha = 0.05) were applied to all regressions.

2.3.3. Resting state analyses

The resting-state analyses aimed at establishing if the regions with altered GM density also showed connectivity patterns that correlated with participants' BMI and task performance. The peaks of each resulting cluster of the VBM analyses were used as seeds for Seed-to-Voxel connectivity analyses. Custom spherical ROIs with a radius of 8 mm centered on each peak were created using the MarsBaR toolbox in Matlab (MARSeille Boîte À Région d'Intérêt, Brett et al., 2002). The behavioral variables that had led to the identification of each peak were used as regressors in the corresponding ROI connectivity analyses (e. g. participants' performance on the bCFS task was used as a regressor in the analysis of the connectivity of the ROIs derived from the VBM on the bCFS task). Following the same approach, the peaks resulting from the VBM analysis, whose regression slope significantly differed in the two groups depending on participants' performance in the bCFS task, were used as seeds in the Seed-to-voxel analysis of the difference in connectivity between high- and low-BMI groups, as predicted by participants' performance at the bCFS task. The same was done for ROIs resulting in the VBM analysis of Go/No-Go task performance. Beta values of the regression slopes were calculated using the REX Matlab toolkit (Duff et al., 2007), and correction for multiple comparisons was applied to all regressions (uncorrected peak level alpha = 0.001, cluster level FDR alpha = 0.05). All analyses included age and gender as covariates of no interest, as done in previous works (see e.g. Smith et al., 2017).

All images were produced using MRIcron software (www.nitrc.org).

3. Results

3.1. bCFS and NoCFS task

3.1.1. Behavioral results

The linear mixed model on the RTs yielded a good fit to the data, explaining 71% of the data variance (marginal $R^2 = 0.64$, conditional $R^2 = 0.71$). Collinearity between factors was calculated using the corvif function in R (HighstatLibV10 library). No predictor showed collinearity with the other predictors (all variance inflation factors between 1 and 2). The results showed a main effect of Task [F (1, 27963) = 58629, $p < 0.001$, $\eta_p^2 = 0.68$], indicating longer RTs in bCFS compared to NoCFS, confirming that suppression had occurred during the bCFS task. Results also showed a significant Task x BMI interaction [F (1, 27943.9) = 226, $p < 0.001$, $\eta_p^2 = 0.01$], depicted in Fig. 2. Higher BMI led to slower RTs in the bCFS task [$p = 0.001$, $\varepsilon_p^2 = 0.17$] but not in the NoCFS task [$p = 0.7$, $\varepsilon_p^2 = -0.02$]. Although the significant difference between bCFS and NoCFS was present in both lower and higher BMIs, it was higher in higher BMIs [lower BMIs $t = 161.5$, $p < 0.001$, $\varepsilon_p^2 = -0.55$; higher BMIs $t = 183.2$, $p < 0.001$, $\varepsilon_p^2 = 0.48$].

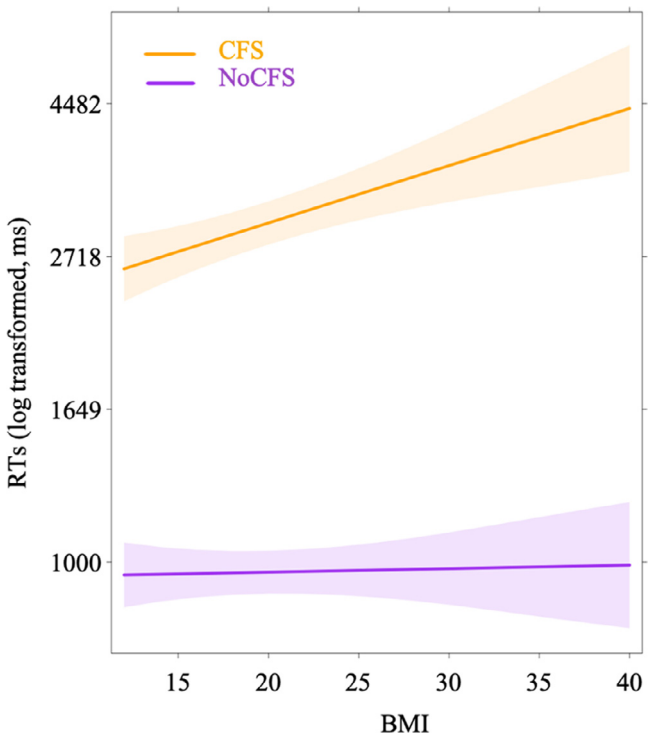

Fig. 2. The interaction effect between Task and BMI. A higher BMI predicts longer RTs in the bCFS task, but not in the NoCFS task. Bands indicate 95% confidence intervals.

Results also showed a significant effect of Task x Stimulus Type [F (1, 27944.7) = 6, $p = 0.016$, $\eta_p^2 = 0.0002$]. Post-hoc tests however failed to find a significant difference between Food and NonFood either in the CFS task ($p = 0.5$, $\varepsilon_p^2 = -0.01$) or in the NoCFS task ($p = 0.7$, $\varepsilon_p^2 = -0.02$), while there was an equally strong effect of Task both in Food trials [$t = 173.3$, $p < 0.001$, $\varepsilon_p^2 = 0.52$] and in NonFood trials [$t = 171.4$, $p < 0.001$, $\varepsilon_p^2 = 0.51$].

In summary, a higher BMI significantly predicted longer RTs in the bCFS task. This effect was irrespective of the Stimulus Category. The complete results are reported in Supplementary Table 3.

3.1.2. Correlation between grey matter density and bCFS task performance independently of BMI

We found a positive correlation between suppression times and GM density in right occipital visual areas (calcarine cortex [$t = 4.92$, $p < 0.001$] and inferior occipital gyrus/occipital fusiform gyrus [$t = 4.04$, $p = 0.007$]) and in the right caudate nucleus [$t = 3.59$, $p = 0.008$], i.e. higher GM density in these areas correlated with longer suppression times. On the other hand, a negative correlation between suppression times and GM density in the left dorsolateral PFC (left middle frontal gyrus [$t = 4.55$, $p = 0.008$]) meant that higher GM density in this prefrontal region correlated with shorter suppression times. Results are reported in Table 2 and depicted in Fig. 3.

3.1.3. Group differences in the correlation between GM density and bCFS task performance

We found that beta values in the correlation between suppression times and GM density were significantly different in the high and low BMI group in the right temporal pole/middle temporal gyrus [$t = 4.18$, $p = 0.002$], in the left orbital gyrus [$t = 4.55$, $p = 0.003$], and in the left operculum and insula [$t = 4.14$, $p = 0.005$]. Beta values indicate that longer suppression times are associated with lower GM density in these areas in the higher BMI group, but not in the lower BMI group.

Results are reported in Table 2 and visually represented in Fig. 4.

Table 2
Neural correlates of bCFS task performance.

H	Brain region	*p* value	Vol (mm^3)	MNI coordinates X	Y	Z	T		
R	Calcarine	< 0.001	2335	16	-84	6	4.92	direct	
R	Inferior Occipital g./Occipital Fusiform g.	0.007	1313	36	-81	-9	4.04	direct	
R	Caudate	0.015	1141	15	0	27	3.59	direct	
L	Middle Frontal g.	0.008	1282	-44	20	34	4.55	indirect	
								***β* lower BMI**	***β* higher BMI**
R	Temporal lobe/Middle Temporal g.	0.002	1573	50	6	-28	4.18	0.019	-0.045
L	Orbital g.	0.003	1542	-27	30	-16	4.55	0.005	-0.044
L	Central operculum/anterior insula	0.005	1384	-36	4	18	4.14	0.007	-0.032
								Seed	
R	Supramarginal G.	0.004	1566	46	-28	32	5.02	right Calcarine/bCFS RTs	
L	Supramarginal G.	0.006	1313	-66	-18	22	5.40	right Calcarine/bCFS RTs	

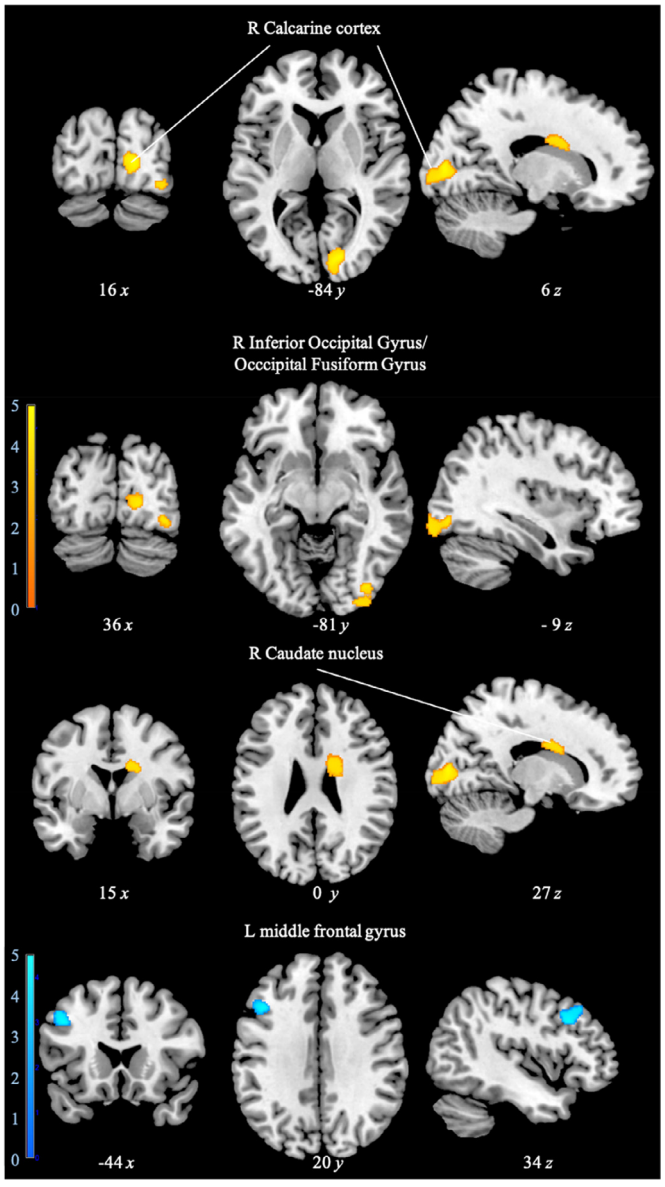

Fig. 3. Sagittal, coronal, and axial view of the position of the clusters in which GMD correlated with mean RTs at the bCFS task. In warm colors, areas in which GM density correlated positively with suppression times in the bCFS task; in cold colors, areas in which GM density correlated inversely with suppression times in the bCFS task. The color scales indicate T values.

3.1.4. BCFS task-related connectivity networks

Longer RTs in the bCFS task correlated with greater connectivity between the right Calcarine ROI and two clusters located in the right and left supramarginal gyri [$t = 5.02$, $p = 0.004$, and $t = 5.40$, $p = 0.006$, respectively], with the left cluster bordering on the postcentral gyrus (see Table 2 and Fig. 5). No other ROI's connectivity was significantly predicted by participants' RTs in the bCFS task.

None of the ROIs resulting from the VBM group analysis of the bCFS task had significantly different connectivity in the higher and lower BMI groups, as predicted by the relative suppression times.

3.2. Go/No-Go task

3.2.1. Behavioral results

The linear mixed model on the RTs of the Go/No-Go task explained 33% of the data variance (marginal $R^2 = 0.01$, conditional $R^2 = 0.33$). No predictor showed collinearity with the other predictors (all variance inflation factors between 1 and 1.001). None of the main effects reached the significance level [all *ps* > 0.12]. We found an interaction effect of Stimulus Type * BMI [F (1, 5306) = 5.3, $p = 0.02$, $\eta_p^2 = 0.001$], shown in Fig. 6. Post-hoc test showed that while BMI did not have a significant effect either in Food or in NonFood trials [all *ps* > 0.07], participants with a higher BMI were slower in responding to NonFood Go trials, i.e. in blocks in which they needed to refrain from responding to food [t (176) = 2.29, $p = 0.02$, $\varepsilon_p^2 = 0.02$], but participants with lower BMIs were not [t (177) = 2.29, $p = 0.57$, $\varepsilon_p^2 = 0$]. This result indicates reduced inhibition in higher BMI participants specifically towards food. Results are reported in Supplementary Table 4.

The model used in the analysis of accuracy explained 33% of the variance (theoretical marginal $R^2 = 0.22$, 0.03; theoretical conditional R^2: 0.33, 0.04). The results showed a main effect of Trials Type ($\chi^2(1) = 189.8$, $p < 0.001$, $\varphi = 0.15$), indicating overall lower accuracy in No-Go trials, and an effect of EAT-26 ($\chi^2(1) = 4.7$, $p = 0.03$, $\varphi = 0.02$), indicating lower accuracy in participants with higher eating disorder symptoms. Complete results are reported in Supplementary Table 5.

3.2.2. Correlation between grey matter density and Go/No-Go task performance independently of BMI

The analysis of RTs in Go trials of the Go/No-Go task showed that faster RTs were associated with higher GM density in the left frontal pole ([$t = 4.41$, $p = 0.002$], see Fig. 7 and Table 3).

Higher accuracy in No-Go trials, i.e. fewer false alarms, correlated with greater GM density in the vermal lobules VIII-X of the right cerebellum ([$t = 3.90$, $p < 0.001$], see Fig. 8 and Table 3). As EAT-26 scores influenced participants' accuracy, we ran a second model covarying EAT-26 scores. This model did not yield any significant correlation between the number of false alarms and GM density.

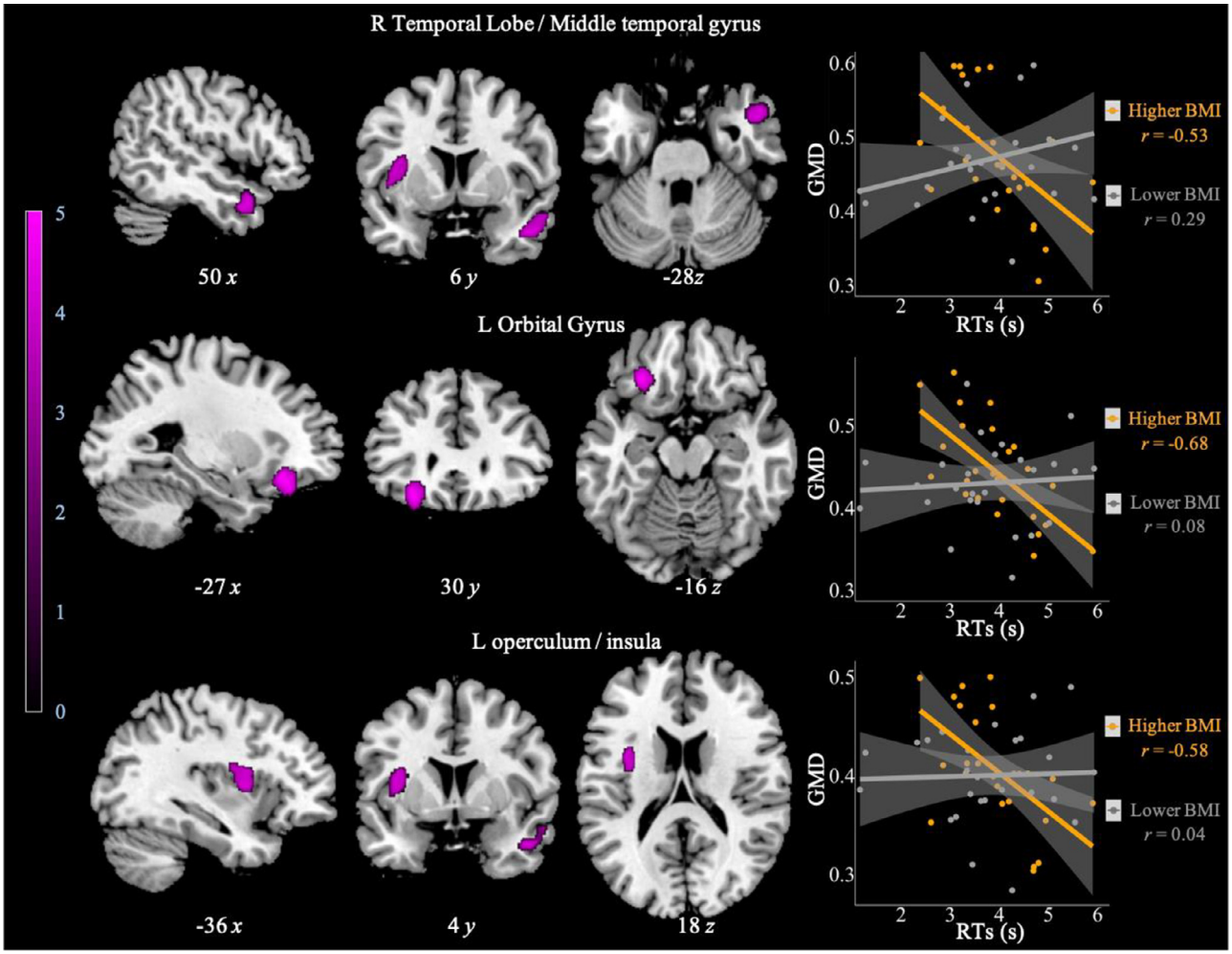

Fig. 4. Sagittal, coronal, and axial view of the position of the clusters in which GMD has a significantly different association with bCFS performance in the higher and lower BMI groups. On the right, for visualization purposes, a scatterplot of the correlation between GMD in each cluster and mean RT in the bCFS task in the higher and lower BMI groups. The color scale indicates T values.

Table 3
Neural correlates of the Go/No-Go task.

H	Brain region	*p* value	Vol (mm^3)	MNI coordinates X	Y	Z	T			
Go/No-Go RTs and GM density										
L	Frontal pole	0.002	1596	-15	75	-4	4.41	direct		
Go/No-Go false alarms and GM density										
R	Cerebellum exterior	< 0.001	2005	4	-63	-39	3.90	indirect		
Go/No-Go RTs and GM density in the higher BMI and lower BMI groups								**β lower BMI**	**β higher BMI**	
R	Parietal operculum	< 0.001	2575	45	-30	22	5.14	0.713	0.471	
L	Orbital g./temporal pole	0.005	1370	-24	27	-32	4.97	-1.037	-0.529	
bCFS RTs and connectivity in the higher and lower BMI groups								**β lower BMI**	**β higher BMI**	**Seed**
L	Precentral/postcentral g.	0.009	1272	-52	-8	22	4.52	3.58	-1.14	R parietal operculum
R	Fusiform gyrus	< 0.001	1478	32	-60	-14	-4.64	-2.52	1.87	L orbital gyrus
R	Lat. occipital cortex	< 0.001	807	32	-70	18	-4.51	-2.15	2.58	L orbital gyrus
L	Lat. occipital cortex	< 0.001	688	-22	-82	26	-4.34	-2.14	2.70	L orbital gyrus

Neural correlates of accuracy on Go trials, i.e. missed targets, were not computed given that accuracy on these trials was very high, as expected when testing healthy participants (mean 99.04%).

3.2.3. Group differences in the correlation between GM density and Go/No-Go task performance

As participants' BMI significantly predicted a food-specific bias in Go trials of the Go/No-Go task, we explored the neural differences in GM density in the higher and lower BMI groups related to the difference between reaction times in nonfood and food trials. We found that a greater difference between nonfood and food trials, i.e. worse performance when inhibiting responses to food compared to nonfood, correlated with lower GM density in the higher BMI group in two areas, the right parietal operculum [$t = 5.14$, $p < 0.001$], and the orbital gyrus/right temporal pole [$t = 4.97$, $p = 0.005$] (see Fig. 9 and Table 3).

Since participants' BMI did not significantly predict their accuracy in the Go/No-Go task, differences in the association between GM density

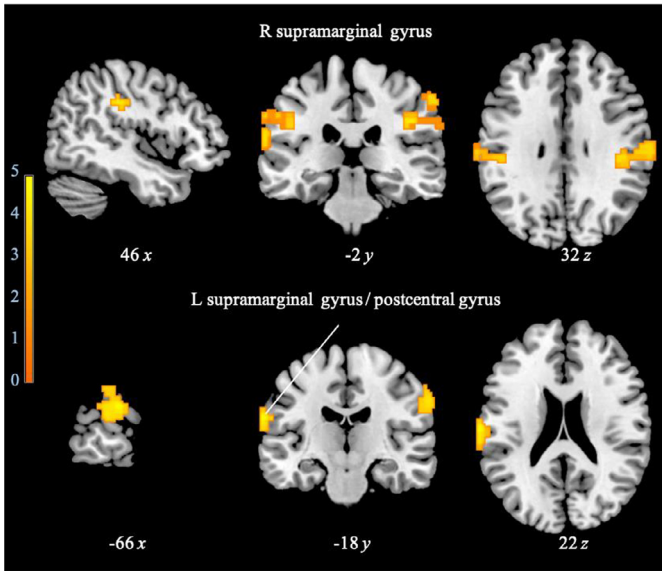

Fig. 5. Sagittal, coronal, and axial view of the position of the clusters whose connectivity with the right Calcarine cortex ROI was predicted by RTs at the bCFS task. The color scale indicates T values.

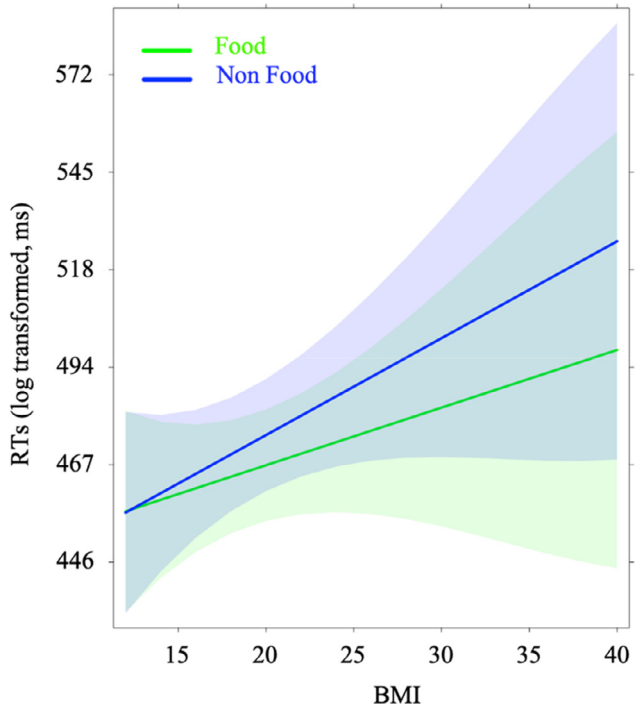

Fig. 6. Interaction effect of BMI and Stimulus Type (Food, NonFood) in the analysis of RTs in the Go/No-Go task. Bands indicate 95% confidence intervals.

and participants' accuracy in the higher and lower BMI groups were not investigated.

3.2.4. Go/No-Go task connectivity networks

In the Go/No-Go task, participants' RTs and accuracy did not predict connectivity between the relative ROIs and the rest of the brain.

Connectivity of the ROIs resulting from the group analysis in the Go/No-Go task as predicted by the difference between nonfood and food go trials indicated that a stronger bias towards food correlated with greater connectivity in the higher BMI group between the right parietal operculum ROI and a cluster located in the left precentral/postcentral

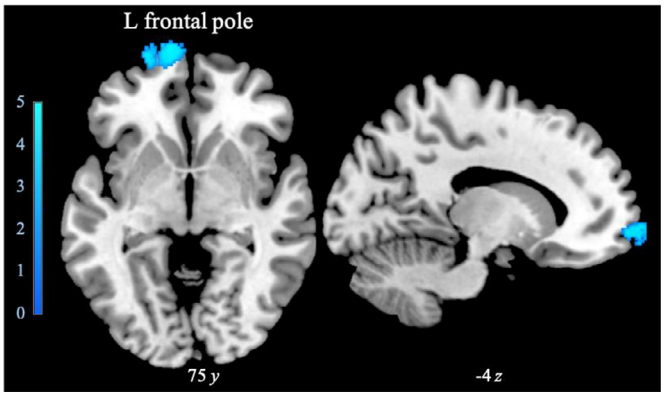

Fig. 7. Coronal and axial view of the cluster in which GM density inversely correlated with RTs in the Go/No-Go task. The color scale indicates T values.

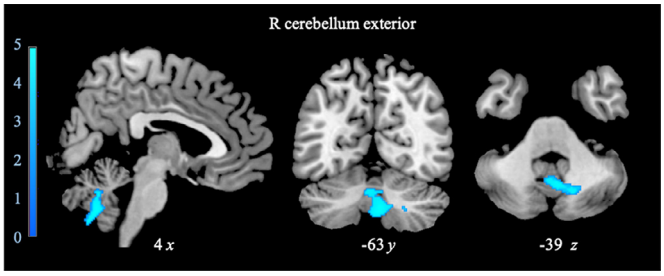

Fig. 8. Sagittal, coronal, and axial view of the position of the cluster whose GMD inversely correlated with the number of false alarms. The color scale indicates T values.

gyri [t = 4.52, p = 0.009], and correlated with lower connectivity between the orbital gyrus ROI and three clusters located in visual areas, namely the right fusiform gyrus [t = -4.64, p < 0.001] and the right and left occipital cortex [t = -4.51, p < 0.001, and t = -4.34, p < 0.001, respectively] (see Fig. 10 and Table 3).

3.3. Neural correlates of BMI

3.3.1. Correlation between grey matter density and BMI

The VBM on BMI (see Supplementary Figure 2 and Supplementary Table 6) showed that participants' BMI positively correlated with GM density in a large subcortical cluster located in the left, and partially right ventral diencephalon, including peaks in the left and right hypothalamus [t = 4.96, p = 0.001].

3.3.2. Body Mass Index ROI connectivity

Higher participants' BMI correlated with lower functional connectivity between the ROI located in the hypothalamus and two clusters located in visual areas, namely a big cluster located between the left lingual gyrus, the bilateral calcarine cortex, and the left cuneal cortex [t = -6.75, p = 0.001], and a smaller cluster located in the left temporal occipital fusiform gyrus [t = -4.76, p = 0.035].

The results are depicted in Supplementary Figure 3 and reported in Supplementary Table 6.

4. Discussion

In this study, we investigated subliminal attentional bias and inhibition toward food in individuals with different BMIs and identified the regions that correlated with individual differences in subliminal processing times and inhibitory performance through brain morphometry and connectivity analyses.

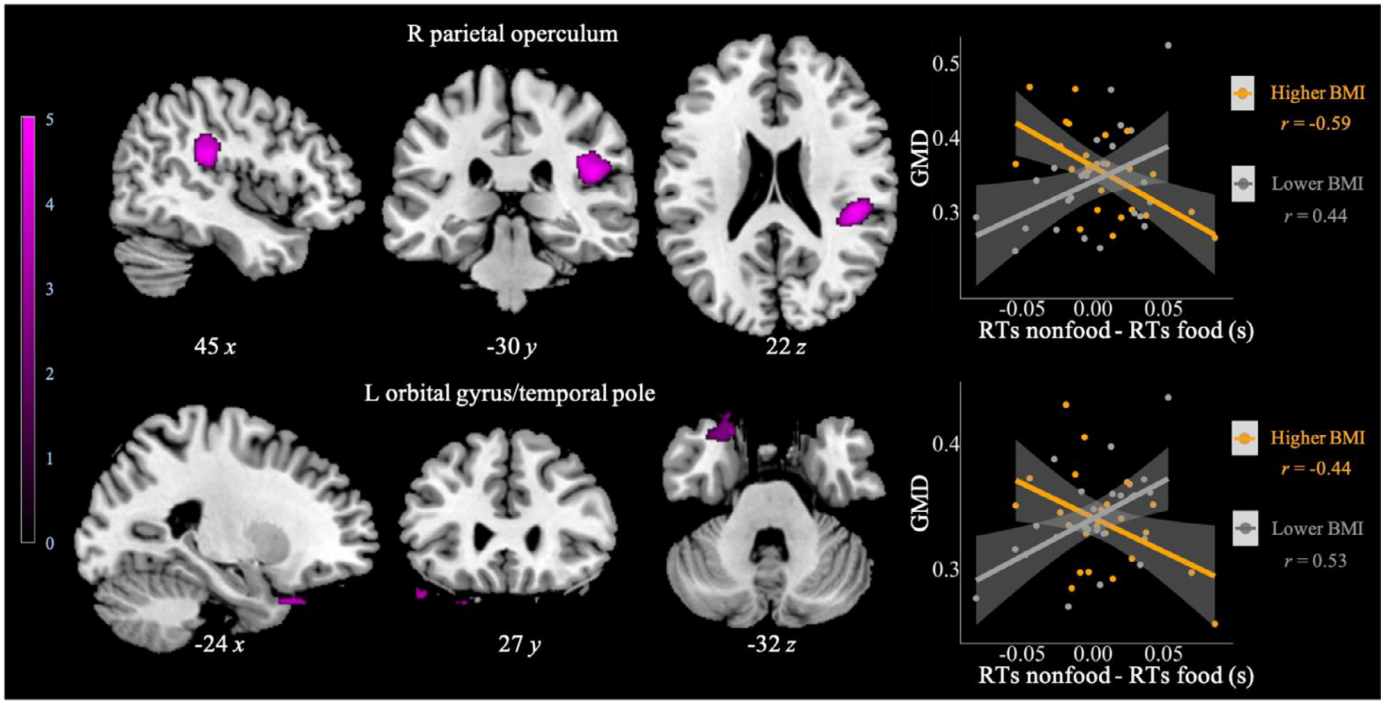

Fig. 9. Sagittal, coronal, and axial view of the clusters in which GM density is predicted differently by the difference between nonfood and food RTs in the higher and lower BMI groups. The color scale indicates T values. On the right, for visualization purposes, a scatterplot of the correlation between GMD in each cluster and the difference in RTs between non-food and food trials of the Go/No-Go task in the higher and lower BMI groups.

4.1. Slower subliminal processing and reduced inhibition towards food in individuals with a higher BMI

In line with our previous study (Osimo et al., 2019), we observed that individuals with a higher BMI showed slower subliminal processing of images than individuals with a lower BMI and that this subliminal processing disadvantage was not specific for food images. Also, individuals with a higher BMI were slower in responding to nonfood go trials than to food go trials in the Go/No-Go task. Slower RTs in nonfood go trials indicate greater difficulty in inhibiting response to food, suggesting a food-specific bias at a later stage of stimulus processing (Meule, 2017). Therefore, the present results confirm that the condition of obesity is not associated with a bias toward food at a subliminal stage of information processing but seems characterized by a domain-general attentional deficit at this stage. This observation complements various findings of general cognitive and attentional deficits in individuals with obesity, while our findings on Go/No-Go task are coherent with the literature that reports lower inhibition towards food images in individuals with overweight and obesity (Kulendran et al., 2017; Price et al., 2015; Svaldi et al., 2015).

4.2. Subliminal processing disadvantages in individuals with a higher BMI are linked to lower GM density in key regions deputed to awareness, high-level sensory integration, and reward

We found that subliminal processing disadvantages in participants with a higher BMI resulted linked to regions implicated in top-down control such as the prefrontal cortex (Osimo et al., 2019), as well as with GM density of brain regions dedicated to awareness, high-level sensory integration, and reward such as the right temporal pole/middle temporal gyrus, the left central operculum and anterior insula, and the left posterior orbital gyrus. Among others, the anterior insula is a key region in awareness (Craig, 2009) and plays a central role in the emotional "salience network" that encodes emotional awareness of cognitive functions and emotionally modulates cognition (Harrison et al., 2010; Seeley et al., 2007). Interestingly, mental slowness in individuals with obesity has recently been found to be associated with an alteration in the salience network (García-García et al., 2013). This is the first study documenting reduced grey matter density associated with the slowness of preconscious processing of stimuli in individuals with obesity, and more studies addressing this issue are needed since subliminal biases have been shown to have a strong influence on appetitive behavior (Finlayson et al., 2008; Forman et al., 2018; Takada et al., 2018).

4.3. Reduced inhibition to food in individuals with a higher BMI is linked to lower GM density in regions implicated in food reward and reduced brain connectivity

Worse performance when inhibiting responses to food compared to nonfood in individuals with a higher BMI in the Go/No-Go task was linked to lower GM density in the right parietal operculum and left orbital gyrus/temporal pole. These areas are implicated in high-level sensory integration but are also associated with food reward and taste processing (Porubská et al., 2006; Beaver et al., 2006; Goldstone et al., 2009; Iannilli et al., 2012; Olson et al., 2007; Van Rijn et al., 2005; Simmons et al., 2005). According to the reward deficit model of obesity (Wang et al., 2002), the reduced GM density in reward regions may stimulate increased intake to compensate for the deficit. Notably, a greater food-specific bias predicted higher connectivity in the higher BMI group between the right parietal operculum and the contralateral precentral gyrus, an area whose activity has been related to the saliency of food stimuli (see for instance Litt et al., 2011) and that has been shown to have increased activation in response to food images in individuals with obesity (Brooks et al., 2013), as well as lower connectivity between the left orbital gyrus and visual areas, i.e. the right fusiform gyrus and the bilateral occipital cortex. Reduced connectivity of visual areas in individuals with a higher BMI is coherent with previous literature results (Zhang et al., 2020), and with the observation that visual areas are activated more strongly by food than by nonfood images, possibly due to greater attentional and motivational salience of food objects

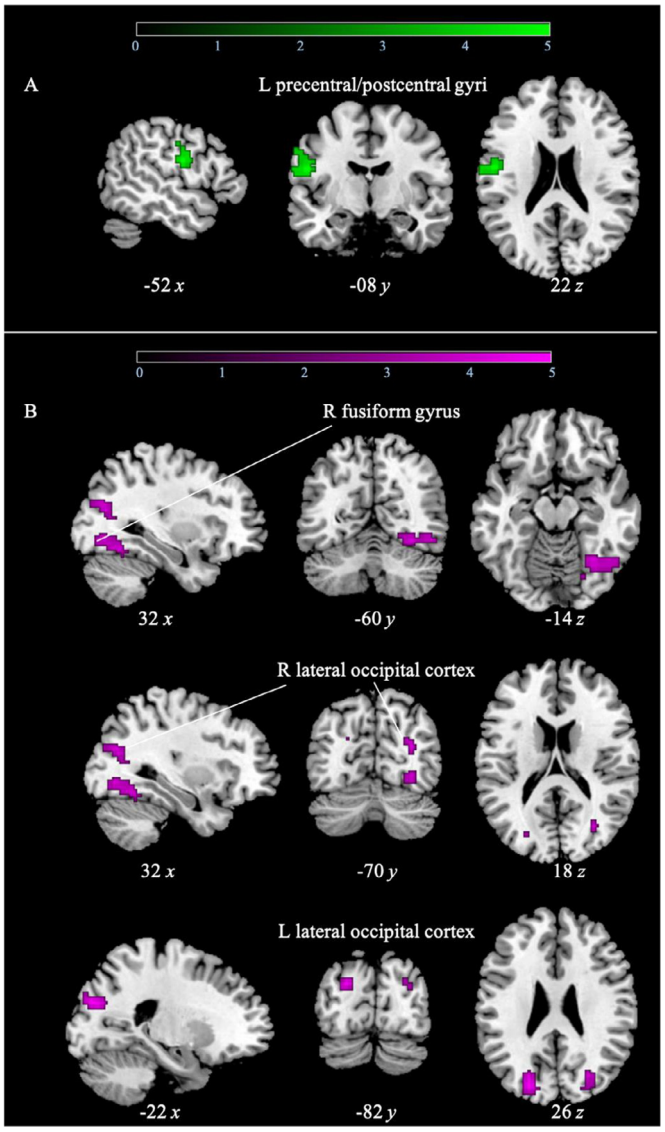

Fig. 10. Sagittal, coronal, and axial view of the position of the ROIs resulting in the connectivity analyses of the Go/No-Go task in the high and low BMI group. In green, the voxels with higher connectivity in the high than in the low BMI group. In violet, the voxels with lower connectivity in the higher than in the lower BMI group. A) Seed: right parietal operculum B) Seed: left orbital gyrus. The color scales indicate T values.

(Adamson and Troiani, 2018; Frank et al., 2010; Masterson et al., 2019; Rosenbaum et al., 2008; van der Laan et al., 2011). Moreover, recognition of food has also been linked with the integrity of occipital areas in patients with dementia (Vignando et al., 2019).

4.4. BMI correlates with GM density in subcortical regions and lower connectivity between the ventral diencephalon and low- and high-level visual areas

Finally, the participants' BMI was found to correlate with GM density in a large subcortical area including the bilateral hypothalamus. Previous studies have associated the state of obesity with subcortical anomalies in the ventral diencephalon (DC) (Marqués-Iturria et al., 2013; Shott et al., 2015). The hypothalamus is a key region in the regulation of appetite (Tataranni et al., 1999), which activates when viewing food stimuli (Killgore et al., 2003). Interestingly, in our study higher BMI also predicted lower connectivity between the ventral DC and low- and high-level visual areas: the left lingual gyrus, the bilateral calcarine cortex, and the left cuneal cortex, and a smaller cluster located in the left temporal occipital fusiform gyrus. Various studies have reported abnormalities in the connectivity of the ventral DC in individuals with overweight/obesity (Baek et al., 2017; Contreras-Rodríguez et al., 2017; García-García et al., 2013; Nummenmaa et al., 2012; Olivo et al., 2016; Park et al., 2015; Steward et al., 2016), as well as reduced connectivity of the fusiform gyri and temporal visual areas (García-García et al., 2015; Kullmann et al., 2013). Lower connectivity between these areas may be linked to a dissociation between perceptive and reward mechanisms, which can be one of the factors leading to overeating in obesity.

4.5. Neural correlates of bCFS suppression times

Independently of BMI, our study provides interesting new evidence regarding structural brain variability associated with the performance in the CFS task. We observed that stronger suppression correlated with higher GM density in low-level (calcarine cortex) and high-level (inferior occipital/occipital fusiform gyri) visual areas. Interestingly, longer suppression times were associated with higher GM density in the right caudate nucleus, a structure implicated in reward-dependent behaviors (Balleine et al., 2007; Nakamura and Hikosaka, 2006). Similarly, Schmack et al. (2016) have found that suppression times can be predicted from activity in visual areas (right fusiform gyrus) and the orbitofrontal cortex. In a review on the neural correlates of arousing subliminal stimuli, Brooks et al. (2012) also found that suppressed arousing stimuli activated the primary visual cortex. Finally, shorter suppression times correlated with higher GM density in the left dorsolateral PFC, an area deputed to top-down control, whose activity is correlated with visual awareness (Dehaene et al., 2006). Therefore, greater attention, inhibition ability, and modulation of the reward circuit are necessary for faster processing of visual stimuli in the bCFS task.

Furthermore, stronger suppression in the bCFS task correlates with higher functional connectivity between visual areas (right calcarine cortex) and two areas located respectively in the right supramarginal gyrus and the left supramarginal and postcentral gyri. It is possible to hypothesize that when visual capture of the visual distractors is coupled with the effort of sensorimotor integration, this can impair the top-down modulation that enables the breaking of the suppressed stimulus into consciousness.

4.6. Neural correlates of reduced inhibition at the Go/No-Go task

Finally, our study also provides interesting results on the neural correlates of good performance in the Go/No-Go task independently of BMI. First, faster RTs in the Go/No-Go task resulted associated with greater GM density in the left frontal pole, an area deputed to high-level monitoring, task switching, and goal-directed behavior (Burgess et al., 2007). A negative association between frontal GM density and performance in the Go/No-Go task was also reported by Li et al. in alcohol-dependent patients (Li et al., 2010). Second, better inhibition, i.e. fewer false alarms, correlated with higher GM density in the right cerebellum. The cerebellum, besides being an important motor area, is implicated in multiple functions, including attention, executive control, and working memory (Strick et al., 2009). Interestingly, it has been found to have a role also in error and conflict processing and response inhibition (Peterburs and Desmond, 2016). This result, however, should be taken with caution, as it disappears when adding the EAT-26 score as a covariate. This suggests that dysfunctional eating habits may influence the relationship between accuracy and GM density in the cerebellum.

4.7. Limitations and future perspectives

Some issues should be acknowledged since they constitute limitations of this study. First, we cannot exclude that the absence of a subliminal attentional bias specific for food stimuli may be due to the composition of the sample, which includes a wide range of BMI but does

not address the presence of a food bias in individuals with overweight vs normal-weight individuals. This choice was made to investigate the effects of BMI as a continuum, but these results may differ in a sample of individuals with higher BMIs. Also, future studies should address how dysfunctional eating attitudes influence subliminal food processing. Second, we did not screen our participants for history of eating disorders, which may have influenced our results. However, we used the EAT-26 scores, which are indicative of eating disorders symptomatology, as covariates in our analyses to isolate the possible effect of eating disorder symptoms. *Third*, it is possible that choosing more salient food stimuli (highly caloric, highly palatable) might have yielded a food-specific subliminal bias. Finally, it is important to note that the Go/No Go task, even if established in the literature, tends to yield small effect sizes that are not always reproduced across studies (Bartholdy et al., 2016; Kulendran et al., 2017).

Given the importance of the temporal aspect of attentional biases, future studies should investigate the neural signature of attentional bias toward food using techniques which allow registering the variation of the neural signal with a better temporal resolution, such as EEG. While fMRI allows for precise spatial resolution and can shed light on the location of the anatomical and functional alterations linked to attentional bias, EEG would allow a more precise analysis of the temporal development of the processing of the signal, which may be of particular interest when studying subliminal biases.

5. Conclusions

In conclusion, this study adds novel findings to the current literature on obesity. It provides the first evidence that individuals with a higher BMI are characterized by slower subliminal processing of visual stimuli and that higher threshold of awareness might be linked to lower GM density of the OFC, bilateral temporal areas, the operculum, and insula. It also confirms reduced inhibition toward food in obesity and shows that the food-specific bias measured through the Go/No-Go task resulted associated with lower GM density in the right parietal operculum and its higher functional connectivity with the left precentral gyrus, lower GM density in the left orbital gyrus/temporal pole, and weaker connectivity with visual areas.

Also, we demonstrated that differences in brain morphology and connectivity are related to different behavioral outcomes at the CFS and the Go/No-Go task. Notably, better behavioral performance at the bCFS and Go/No-Go tasks correlates with higher GM density in frontal control areas, while slower subliminal processing is linked to higher GM density in areas involved in visual processing and reward, as well as to higher connectivity to sensorimotor areas and lower connectivity to visual areas.

These results indicate that a specific bias towards food is present only at a late, conscious stage of visual processing, and is associated with lower GM density in reward brain regions. In addition, our results indicate that a higher BMI is also associated with slower visual processing in its early, subliminal stages, although not specifically for food stimuli, and that this slower processing is linked to morphological alterations of key areas involved in awareness, high-level sensory integration, and reward. In addition, independently of the kind of stimuli used, our results indicated that behavioral alterations in the performance of the bCFS and Go/No-Go task can be attributed to alterations in the reward and control circuits. These tasks should therefore be considered useful proxies for the implicit evaluation of reward and control functions.

Declaration of Competing Interest

None.

Acknowledgments

The authors thank Carol Coricelli for her comments and insights on a previous version of this paper and Maria (Nina) Bullard for the English revision of the manuscript.

Data/code availability statement

The behavioral and neuroimaging data is available at this address: https://osf.io/8vgzu/?view_only=9605d16738294ac490ca8be786264bd7

Supplementary materials

Supplementary material associated with this article can be found, in the online version, at doi:10.1016/j.neuroimage.2021.117725.

References

Adamson, K., Troiani, V., 2018. Distinct and overlapping fusiform activation to faces and food. NeuroImage 174, 393–406. doi:10.1016/j.neuroimage.2018.02.064.

Aiello, M., Ambron, E., Situlin, R., Foroni, F., Biolo, G., Rumiati, R.I., 2018. Body weight and its association with impulsivity in middle and old age individuals. Brain Cogn. 123, 103–109. doi:10.1016/j.bandc.2018.03.006.

Aiello, M., Eleopra, R., Foroni, F., Rinaldo, S., Rumiati, R.I., 2017. Weight gain after STN-DBS: The role of reward sensitivity and impulsivity. Cortex 92, 150–161. doi:10.1016/j.cortex.2017.04.005.

Anstine, D., Grinenko, D., 2000. Rapid screening for disordered eating in college-aged females in the primary care setting. J. Adolesc. Health 26, 338–342. doi:10.1016/S1054-139X(99)00120-2.

Baek, K., Morris, L.S., Kundu, P., Voon, V., 2017. Disrupted resting-state brain network properties in obesity: decreased global and putaminal cortico-striatal network efficiency. Psychol. Med. 47, 585–596. doi:10.1017/S0033291716002646.

Balleine, B.W., Delgado, M.R., Hikosaka, O., 2007. The role of the dorsal striatum in reward and decision-making. J. Neurosci. 27, 8161–8165. doi:10.1523/JNEUROSCI.1554-07.2007.

Bar-Haim, Y., Lamy, D., Pergamin, L., Bakermans-Kranenburg, M.J., van IJzendoorn, M.H., 2007. Threat-related attentional bias in anxious and nonanxious individuals: A meta-analytic study. Psychol. Bull. 133, 1–24. doi:10.1037/0033-2909.133.1.1.

Bartholdy, S., Dalton, B., O'Daly, O.G., Campbell, I.C., Schmidt, U., 2016. A systematic review of the relationship between eating, weight and inhibitory control using the stop signal task. Neurosci. Biobehav. Rev. 64, 35–62. doi:10.1016/j.neubiorev.2016.02.010.

Barton, K., 2020. MuMIn.

Bates, D., Mächler, M., Bolker, B., Walker, S., 2015. Fitting linear mixed-effects models using lme4. J. Stat. Softw. 67. doi:10.18637/jss.v067.i01.

Batterink, L., Yokum, S., Stice, E., 2010. Body mass correlates inversely with inhibitory control in response to food among adolescent girls: an fMRI study. NeuroImage 52, 1696–1703. doi:10.1016/j.neuroimage.2010.05.059.

Beaver, J.D., Lawrence, A.D., van Ditzhuijzen, J., Davis, M.H., Woods, A., Calder, A.J., 2006. Individual differences in reward drive predict neural responses to images of food. J. Neurosci. Off. J. Soc. Neurosci. 26, 5160–5166. doi:10.1523/JNEUROSCI.0350-06.2006.

Ben-Shachar, M.S., Makowski, D., Lüdecke, D., Patil, I., Kelley, K., Stanley, D., 2020. effectsize.

Bogler, C., Bode, S., Haynes, J.-D., 2011. Decoding successive computational stages of saliency processing. Curr. Biol. 21, 1667–1671. doi:10.1016/j.cub.2011.08.039.

Bolker, B.M., Brooks, M.E., Clark, C.J., Geange, S.W., Poulsen, J.R., Stevens, M.H.H., White, J.-S.S., 2009. Generalized linear mixed models: a practical guide for ecology and evolution. Trends Ecol. Evol. 24, 127–135. doi:10.1016/j.tree.2008.10.008.

Brett, M., Anton, J.-L., Valabregue, R., Poline, J.-B., 2002. Region of interest analysis using an SPM toolbox. In: Proceedings of the 8th International Conference on Functional Mapping of the Human Brain. Sendau, Japan. NeuroImage.

Brooks, S.J., Cedernaes, J., Schiöth, H.B., 2013. Increased prefrontal and parahippocampal activation with reduced dorsolateral prefrontal and insular cortex activation to food images in obesity: a meta-analysis of fMRI studies. PLOS ONE 8, e60393. doi:10.1371/journal.pone.0060393.

Brooks, S.J., Prince, A., Stahl, D., Campbell, I.C., Treasure, J., 2011. A systematic review and meta-analysis of cognitive bias to food stimuli in people with disordered eating behaviour. Clin. Psychol. Rev. 31, 37–51. doi:10.1016/j.cpr.2010.09.006.

Brooks, S.J., Savov, V., Allzén, E., Benedict, C., Fredriksson, R., Schiöth, H.B., 2012. Exposure to subliminal arousing stimuli induces robust activation in the amygdala, hippocampus, anterior cingulate, insular cortex and primary visual cortex: a systematic meta-analysis of fMRI studies. NeuroImage 59, 2962–2973. doi:10.1016/j.neuroimage.2011.09.077.

Burgess, P.W., Dumontheil, I., Gilbert, S.J., 2007. The gateway hypothesis of rostral prefrontal cortex (area 10) function. Trends Cogn. Sci. 11, 290–298. doi:10.1016/j.tics.2007.05.004.

Calitri, R., Pothos, E.M., Tapper, K., Brunstrom, J.M., Rogers, P.J., 2010. Cognitive biases to healthy and unhealthy food words predict change in BMI. Obes. Silver Spring Md 18, 2282–2287. doi:10.1038/oby.2010.78.

Capitão, L.P., Underdown, S.J.V., Vile, S., Yang, E., Harmer, C.J., Murphy, S.E., 2014. Anxiety increases breakthrough of threat stimuli in continuous flash suppression. Emot. Wash. DC 14, 1027–1036. doi:10.1037/a0037801.

Castellanos, E.H., Charboneau, E., Dietrich, M.S., Park, S., Bradley, B.P., Mogg, K., Cowan, R.L., 2009. Obese adults have visual attention bias for food cue images: evidence for altered reward system function. Int. J. Obes. 33, 1063–1073. doi:10.1038/ijo.2009.138, 2005.

Contreras-Rodríguez, O., Martín-Pérez, C., Vilar-López, R., Verdejo-Garcia, A., 2017. Ventral and dorsal striatum networks in obesity: link to food craving and weight gain. Biol. Psychiatry, Obesity and Food Addict. 81, 789–796. doi:10.1016/j.biopsych.2015.11.020.

Craig, A.D.(Bud), 2009. How do you feel — now? The anterior insula and human awareness. Nat. Rev. Neurosci. 10, 59–70. doi:10.1038/nrn2555.

Cserjesi, R., Vos, I.D., Deroost, N., 2016. Discrepancy between implicit and explicit preferences for food portions in obesity. Int. J. Obes. 40, 1464–1467. doi:10.1038/ijo.2016.91.

Dehaene, S., Changeux, J.-P., 2011. Experimental and theoretical approaches to conscious processing. Neuron 70, 200–227. doi:10.1016/j.neuron.2011.03.018.

Dehaene, S., Changeux, J.-P., Naccache, L., Sackur, J., Sergent, C., 2006. Conscious, preconscious, and subliminal processing: a testable taxonomy. Trends Cogn. Sci. 10, 204–211. doi:10.1016/j.tics.2006.03.007.

Dotti, A., Lazzari, R., 1998. Validation and reliability of the Italian EAT-26. Eat. Weight Disord. EWD 3, 188–194.

Draper, N.R., Smith, H., 1998. Applied Regression Analysis. John Wiley & Sons.

Duff, E.P., Cunnington, R., Egan, G.F., 2007. REX: response exploration for neuroimaging datasets. Neuroinformatics 5, 223–234. doi:10.1007/s12021-007-9001-y.

Fang, F., He, S., 2005. Cortical responses to invisible objects in the human dorsal and ventral pathways. Nat. Neurosci. 8, 1380–1385. doi:10.1038/nn1537.

Field, M., Cox, W.M., 2008. Attentional bias in addictive behaviors: A review of its development, causes, and consequences. Drug Alcohol Depend. 97, 1–20. doi:10.1016/j.drugalcdep.2008.03.030.

Finlayson, G., King, N., Blundell, J., 2008. The role of implicit wanting in relation to explicit liking and wanting for food: Implications for appetite control. Appetite 50, 120–127. doi:10.1016/j.appet.2007.06.007.

Forman, E.M., Goldstein, S.P., Flack, D., Evans, B.C., Manasse, S.M., Dochat, C., 2018. Promising technological innovations in cognitive training to treat eating-related behavior. Appetite, Executive Funct. Train. Eat. Behav. 124, 68–77. doi:10.1016/j.appet.2017.04.011.

Foroni, F., Pergola, G., Argiris, G., Rumiati, R.I., 2013. The FoodCast research image database (FRIDa). Front. Hum. Neurosci. 7, 51. doi:10.3389/fnhum.2013.00051.

Fox, J., Weisberg, S., 2019. An {R} Companion to Applied Regression, Third Edition Sage, Thousand Oaks CA ed.

Frank, S., Laharnar, N., Kullmann, S., Veit, R., Canova, C., Hegner, Y.L., Fritsche, A., Preissl, H., 2010. Processing of food pictures: influence of hunger, gender and calorie content. Brain Res., Neural Mech. Ingest. Behav. Obes. 1350, 159–166. doi:10.1016/j.brainres.2010.04.030.

Friston, K.J., Ashburner, J., Heather, J., Holmes, A., Poline, J.-B., 2017. SPM - Statistical Parametric Mapping. The MathWorks, Inc., Natick, Massachusetts, United States.

García-García, I., Jurado, M.Á., Garolera, M., Marqués-Iturria, I., Horstmann, A., Segura, B., Pueyo, R., Sender-Palacios, M.J., Vernet-Vernet, M., Villringer, A., Junqué, C., Margulies, D.S., Neumann, J., 2015. Functional network centrality in obesity: a resting-state and task fMRI study. Psychiatry Res. Neuroimaging 233, 331–338. doi:10.1016/j.pscychresns.2015.05.017.

García-García, I., Jurado, M.Á., Garolera, M., Segura, B., Sala-Llonch, R., Marqués-Iturria, I., Pueyo, R., Sender-Palacios, M.J., Vernet-Vernet, M., Narberhaus, A., Ariza, M., Junqué, C., 2013. Alterations of the salience network in obesity: a resting-state fMRI study. Hum. Brain Mapp. 34, 2786–2797. doi:10.1002/hbm.22104.

Garner, D.M., Olmsted, M.P., Bohr, Y., Garfinkel, P.E., 1982. The eating attitudes test: psychometric features and clinical correlates. Psychol. Med. 12, 871–878. doi:10.1017/S0033291700049163.

Gaser, C., Danhke, R., 2016. CAT - Computational Anatomy Toolbox for SPM. The MathWorks, Inc., Natick, Massachusetts, United States.

Gayet, S., Van der Stigchel, S., Paffen, C.L.E., 2014. Breaking continuous flash suppression: competing for consciousness on the pre-semantic battlefield. Front. Psychol. 5. doi:10.3389/fpsyg.2014.00460.

Goldstone, A.P., Prechtl de Hernandez, C.G., Beaver, J.D., Muhammed, K., Croese, C., Bell, G., Durighel, G., Hughes, E., Waldman, A.D., Frost, G., Bell, J.D., 2009. Fasting biases brain reward systems towards high-calorie foods. Eur. J. Neurosci. 30, 1625–1635. doi:10.1111/j.1460-9568.2009.06949.x.

Gray, K.L.H., Adams, W.J., Hedger, N., Newton, K.E., Garner, M., 2013. Faces and awareness: low-level, not emotional factors determine perceptual dominance. Emot. Wash. DC 13, 537–544. doi:10.1037/a0031403.

Harrison, N.A., Gray, M.A., Gianaros, P.J., Critchley, H.D., 2010. The embodiment of emotional feelings in the brain. J. Neurosci. Off. J. Soc. Neurosci. 30, 12878–12884. doi:10.1523/JNEUROSCI.1725-10.2010.

Hendrikse, J.J., Cachia, R.L., Kothe, E.J., McPhie, S., Skouteris, H., Hayden, M.J., 2015. Attentional biases for food cues in overweight and individuals with obesity: a systematic review of the literature. Obes. Rev. Off. J. Int. Assoc. Study Obes. 16, 424–432. doi:10.1111/obr.12265.

Iannilli, E., Singh, P.B., Schuster, B., Gerber, J., Hummel, T., 2012. Taste laterality studied by means of umami and salt stimuli: an fMRI study. NeuroImage 60, 426–435. doi:10.1016/j.neuroimage.2011.12.088.

Kemps, E., Tiggemann, M., 2015. Approach bias for food cues in obese individuals. Psychol. Health 30, 370–380. doi:10.1080/08870446.2014.974605.

Killgore, W.D.S., Young, A.D., Femia, L.A., Bogorodzki, P., Rogowska, J., Yurgelun-Todd, D.A., 2003. Cortical and limbic activation during viewing of high- versus low-calorie foods. NeuroImage 19, 1381–1394. doi:10.1016/S1053-8119(03)00191-5.

Kulendran, M., Vlaev, I., Gamboa, P., Darzi, A., 2017. The role of impulsivity in obesity as measured by inhibitory control: a systematic review. Med. Res. Arch. 5.

Kullmann, S., Pape, A.-A., Heni, M., Ketterer, C., Schick, F., Häring, H.-U., Fritsche, A., Preissl, H., Veit, R., 2013. Functional network connectivity underlying food processing: disturbed salience and visual processing in overweight and obese adults. Cereb. Cortex N. Y. N 1991 (23), 1247–1256. doi:10.1093/cercor/bhs124.

Kuznetsova, A., Brockhoff, P.B., Christensen, R.H.B., 2017. lmerTest package: tests in linear mixed effects models. J. Stat. Softw. 82. doi:10.18637/jss.v082.i13.

Li, C.-T., Lin, C.-P., Chou, K.-H., Chen, I.-Y., Hsieh, J.-C., Wu, C.-L., Lin, W.-C., Su, T.-P., 2010. Structural and cognitive deficits in remitting and non-remitting recurrent depression: a voxel-based morphometric study. NeuroImage 50, 347–356. doi:10.1016/j.neuroimage.2009.11.021.

Litt, A., Plassmann, H., Shiv, B., Rangel, A., 2011. Dissociating valuation and saliency signals during decision-making. Cereb. Cortex N. Y. N 1991 (21), 95–102. doi:10.1093/cercor/bhq065.

Loeber, S., Grosshans, M., Herpertz, S., Kiefer, F., Herpertz, S.C., 2013. Hunger modulates behavioral disinhibition and attention allocation to food-associated cues in normal-weight controls. Appetite 71, 32–39. doi:10.1016/j.appet.2013.07.008.

Marqués-Iturria, I., Pueyo, R., Garolera, M., Segura, B., Junqué, C., García-García, I., José Sender-Palacios, M., Vernet-Vernet, M., Narberhaus, A., Ariza, M., Jurado, M.Á., 2013. Frontal cortical thinning and subcortical volume reductions in early adulthood obesity. Psychiatry Res. Neuroimaging 214, 109–115. doi:10.1016/j.pscychresns.2013.06.004.

Masterson, T.D., Stein, W.M., Beidler, E., Bermudez, M., English, L.K., Keller, K.L., 2019. Brain response to food brands correlates with increased intake from branded meals in children: an fMRI study. Brain Imaging Behav. 13, 1035–1048. doi:10.1007/s11682-018-9919-8.

Meule, A., 2017. Reporting and interpreting task performance in go/no-go affective shifting tasks. Front. Psychol. 8. doi:10.3389/fpsyg.2017.00701.

Nakamura, K., Hikosaka, O., 2006. Role of dopamine in the primate caudate nucleus in reward modulation of saccades. J. Neurosci. Off. J. Soc. Neurosci. 26, 5360–5369. doi:10.1523/JNEUROSCI.4853-05.2006.

Nummenmaa, L., Hirvonen, J., Hannukainen, J.C., Immonen, H., Lindroos, M.M., Salminen, P., Nuutila, P., 2012. Dorsal striatum and its limbic connectivity mediate abnormal anticipatory reward processing in obesity. PLoS ONE 7. doi:10.1371/journal.pone.0031089.

Olivo, G., Wiemerslage, L., Nilsson, E.K., Solstrand Dahlberg, L., Larsen, A.L., Olaya Búcaro, M., Gustafsson, V.P., Titova, O.E., Bandstein, M., Larsson, E.-M., Benedict, C., Brooks, S.J., Schiöth, H.B., 2016. Resting-state brain and the FTO obesity risk allele: default mode, sensorimotor, and salience network connectivity underlying different somatosensory integration and reward processing between genotypes. Front. Hum. Neurosci. 10. doi:10.3389/fnhum.2016.00052.

Olson, I.R., Plotzker, A., Ezzyat, Y., 2007. The Enigmatic temporal pole: a review of findings on social and emotional processing. Brain 130, 1718–1731. doi:10.1093/brain/awm052.

Osimo, S.A., Korb, S., Aiello, M., 2019. Obesity, subliminal perception and inhibition: neuromodulation of the prefrontal cortex. Behav. Res. Ther. doi:10.1016/j.brat.2019.05.005.

Park, B., Seo, J., Yi, J., Park, H., 2015. Structural and functional brain connectivity of people with obesity and prediction of body mass index using connectivity. PLoS ONE 10. doi:10.1371/journal.pone.0141376.

Peirce, J.W., 2007. PsychoPy—Psychophysics software in Python. J. Neurosci. Methods 162, 8–13. doi:10.1016/j.jneumeth.2006.11.017.

Peterburs, J., Desmond, J.E., 2016. The role of the human cerebellum in performance monitoring. Curr. Opin. Neurobiol. 40, 38–44. doi:10.1016/j.conb.2016.06.011.

Porubská, K., Veit, R., Preissl, H., Fritsche, A., Birbaumer, N., 2006. Subjective feeling of appetite modulates brain activity: An fMRI study. NeuroImage 32, 1273–1280. doi:10.1016/j.neuroimage.2006.04.216.

Price, M., Lee, M., Higgs, S., 2015. Food-specific response inhibition, dietary restraint and snack intake in lean and overweight/obese adults: a moderated-mediation model. Int. J. Obes. 40 (1), 6. doi:10.1038/ijo.2015.235.

R Core Team, 2017. R: A Language and Environment for Statistical Computing. R Foundation for Statistical Computing, Vienna, Austria.

Rosenbaum, M., Sy, M., Pavlovich, K., Leibel, R.L., Hirsch, J., 2008. Leptin reverses weight loss–induced changes in regional neural activity responses to visual food stimuli. J. Clin. Invest. 118, 2583–2591. doi:10.1172/JCI35055.

Schmack, K., Burk, J., Haynes, J.-D., Sterzer, P., 2016. Predicting subjective affective salience from cortical responses to invisible object stimuli. Cereb. Cortex 26, 3453–3460. doi:10.1093/cercor/bhv174.

Schulz, K.P., Fan, J., Magidina, O., Marks, D.J., Hahn, B., Halperin, J.M., 2007. Does the emotional go/no-go task really measure behavioral inhibition? Convergence with measures on a non-emotional analog. Arch. Clin. Neuropsychol. 22, 151–160. doi:10.1016/j.acn.2006.12.001.

Seeley, W.W., Menon, V., Schatzberg, A.F., Keller, J., Glover, G.H., Kenna, H., Reiss, A.L., Greicius, M.D., 2007. Dissociable intrinsic connectivity networks for salience processing and executive control. J. Neurosci. Off. J. Soc. Neurosci. 27, 2349–2356. doi:10.1523/JNEUROSCI.5587-06.2007.

Shott, M.E., Cornier, M.-A., Mittal, V.A., Pryor, T.L., Orr, J.M., Brown, M.S., Frank, G.K.W., 2015. Orbitofrontal cortex volume and brain reward response in obesity. Int. J. Obes. 2005 (39), 214–221. doi:10.1038/ijo.2014.121.

Simmons, W.K., Martin, A., Barsalou, L.W., 2005. Pictures of appetizing foods activate gustatory cortices for taste and reward. Cereb. Cortex 15, 1602–1608. doi:10.1093/cercor/bhi038.

Smith, R., Alkozei, A., Bao, J., Smith, C., Lane, R.D., Killgore, W.D.S., 2017. Resting state functional connectivity correlates of emotional awareness. NeuroImage 159, 99–106. doi:10.1016/j.neuroimage.2017.07.044.

Sterzer, P., Haynes, J.-D., Rees, G., 2008. Fine-scale activity patterns in high-level visual areas encode the category of invisible objects. J. Vis. 8. doi:10.1167/8.15.10, 10–10.

Steward, T., Picó-Pérez, M., Mata, F., Martínez-Zalacaín, I., Cano, M., Contreras-Rodríguez, O., Fernández-Aranda, F., Yucel, M., Soriano-Mas, C., Verdejo-García, A., 2016. Emotion regulation and excess weight: impaired affective processing characterized by dysfunctional insula activation and connectivity. PLoS ONE 11. doi:10.1371/journal.pone.0152150.

Straube, T., Mentzel, H.-J., Miltner, W.H.R., 2006. Neural mechanisms of automatic and direct processing of phobogenic stimuli in specific phobia. Biol. Psychiatry 59, 162–170. doi:10.1016/j.biopsych.2005.06.013.

Strick, P.L., Dum, R.P., Fiez, J.A., 2009. Cerebellum and nonmotor function. Annu. Rev. Neurosci. 32, 413–434. doi:10.1146/annurev.neuro.31.060407.125606.

Svaldi, J., Naumann, E., Biehl, S., Schmitz, F., 2015. Impaired early-response inhibition in overweight females with and without binge eating disorder. PLOS ONE 10, e0133534. doi:10.1371/journal.pone.0133534.

Takada, K., Ishii, A., Matsuo, T., Nakamura, C., Uji, M., Yoshikawa, T., 2018. Neural activity induced by visual food stimuli presented out of awareness: a preliminary magnetoencephalography study. Sci. Rep. 8, 3119. doi:10.1038/s41598-018-21383-0.

Tataranni, P.A., Gautier, J.F., Chen, K., Uecker, A., Bandy, D., Salbe, A.D., Pratley, R.E., Lawson, M., Reiman, E.M., Ravussin, E., 1999. Neuroanatomical correlates of hunger and satiation in humans using positron emission tomography. Proc. Natl. Acad. Sci. U. S. A. 96, 4569–4574.

Tsuchiya, N., Koch, C., 2005. Continuous flash suppression reduces negative afterimages. Nat. Neurosci. 8, 1096–1101. doi:10.1038/nn1500.

van der Laan, L.N., de Ridder, D.T.D., Viergever, M.A., Smeets, P.a.M., 2011. The first taste is always with the eyes: a meta-analysis on the neural correlates of processing visual food cues. NeuroImage 55, 296–303. doi:10.1016/j.neuroimage.2010.11.055.

Van Rijn, S., Aleman, A., Van Diessen, E., Berckmoes, C., Vingerhoets, G., Kahn, R.S., 2005. What is said or how it is said makes a difference: role of the right fronto-parietal operculum in emotional prosody as revealed by repetitive TMS. Eur. J. Neurosci. 21, 3195–3200. doi:10.1111/j.1460-9568.2005.04130.x.

Veenstra, E.M., de Jong, P.J., Koster, E.H.W., Roefs, A., 2010. Attentional avoidance of high-fat food in unsuccessful dieters. J. Behav. Ther. Exp. Psychiatry 41, 282–288. doi:10.1016/j.jbtep.2010.02.006.

Vignando, M., Aiello, M., Rinaldi, A., Cattarruzza, T., Mazzon, G., Manganotti, P., Eleopra, R., Rumiati, R.I., 2019. Food knowledge depends upon the integrity of both sensory and functional properties: a VBM, TBSS and DTI tractography study. Sci. Rep. 9, 7439. doi:10.1038/s41598-019-43919-8.

Wang, G.-J., Volkow, N.D., Fowler, J.S., 2002. The role of dopamine in motivation for food in humans: implications for obesity. Expert Opin. Ther. Targets 6, 601–609. doi:10.1517/14728222.6.5.601.

Werthmann, J., Jansen, A., Roefs, A., 2015. Worry or craving? A selective review of evidence for food-related attention biases in obese individuals, eating-disorder patients, restrained eaters and healthy samples. Proc. Nutr. Soc. 74, 99–114. doi:10.1017/S0029665114001451.

Whitfield-Gabrieli, S., Nieto-Castanon, A., 2012. Conn: a functional connectivity toolbox for correlated and anticorrelated brain networks. Brain Connect. 2, 125–141. doi:10.1089/brain.2012.0073.

Yang, E., Blake, R., 2012. Deconstructing continuous flash suppression. J. Vis. 12, 8. doi:10.1167/12.3.8.

Yang, Z., Zhao, J., Jiang, Y., Li, C., Wang, J., Weng, X., Northoff, G., 2011. Altered negative unconscious processing in major depressive disorder: an exploratory neuropsychological study. PLOS ONE 6, e21881. doi:10.1371/journal.pone.0021881.

Yuval-Greenberg, S., Heeger, D.J., 2013. Continuous flash suppression modulates cortical activity in early visual cortex. J. Neurosci. 33, 9635–9643. doi:10.1523/JNEUROSCI.4612-12.2013.

Zhang, P., Wu, G., Yu, F., Liu, Y., Li, M., Wang, Zheng, Ding, H., Li, X., Wang, H., Jin, M., Zhang, Zheng-yu, Zhao, P., Li, J., Yang, Z., Lv, H., Zhang, Zhong-tao, Wang, Zhen-chang, 2020. Abnormal regional neural activity and reorganized neural network in obesity: evidence from resting-state fMRI. Obesity 28, 1283–1291. doi:10.1002/oby.22839.

Zhang, S., Cui, L., Sun, X., Zhang, Q., 2018. The effect of attentional bias modification on eating behavior among women craving high-calorie food. Appetite 129, 135–142. doi:10.1016/j.appet.2018.07.004.